

## Effects of Co doping on the magnetic properties of Fe<sub>2</sub>O<sub>3</sub> nanoparticles

Y. Ichiyanagi, J. Yamazaki, Y. Kimishima and Y. Tachibana

Graduate School of Engineering, Yokohama National University,

79-5 Tokiwadai, Hodogaya, Yokohama 240-8501 Japan,

Fax:81-45-339-4185, e-mail:yuko@ynu.ac.jp

Magnetization measurements were performed on Co doped Fe<sub>2</sub>O<sub>3</sub> nanoparticles in a field of  $\pm 5T$  and a temperature range from 5 K to 300 K. The mole ratio of Co/Fe was varied between 0.05 and 0.7. Magnetic parameters were not always proportional to the Co ionic concentration. With a measuring temperature of 100 K, coersivity began to increase dramatically as the amount of Co ion increased; however, the largest coersivity was observed near a Co/Fe ratio of 0.4, and it then relatively constant at higher concentrations. This tendency might be attributed to the formation of newly produced CoFe<sub>2</sub>O<sub>4</sub> (Co-ferrite) nanoparticles at that ratio, instead of  $\gamma$ -Fe<sub>2</sub>O<sub>3</sub>, which was dominant in the Fe-rich region. A lack of further increase in coersivity at higher concentrations of Co ion could be due to the production of antiferromagnetic CoO particles in the Co-rich region. Correlations between particle sizes and blocking temperatures are also discussed.

Key words: magnetization, nanoparticles, iron oxide, cobalt ferrite

### 1. INTRODUCTION

Magnetic nanoparticles have attracted increasing interest, not only for their remarkable nanoscopic phenomena, but also from the aspect of industrial applications. The authors have reported magnetic properties of Ni(OH)<sub>2</sub> monolayer nanoclusters (Ni-MNC) encapsulated in a silica cage [1][2][3][4][5]. Ni-MNC has ferromagnetic transition temperature at  $T_C = 10$  K while bulk crystal has  $T_N = 25.75$  K [6]. The properties of Ni-MNC were found to be between a spin glass system and superparamagnetic system from the various parameters, and quantum tunneling of magnetization (QMT) was also observed below  $T_C$  [4]. NiO nanoparticles with average sizes ranging from 2.0 to 5.4 nm were also produced. These NiO particles exhibited slight hysteretic behavior below 20 K [7] though the Néel temperature of the bulk crystal was known to be  $T_N = 523$  K.

Recently, the authors have successfully obtained Fe<sub>2</sub>O<sub>3</sub> nanoparticles by the same method as that used previously for Ni(OH)<sub>2</sub> [8]. The diameters of these clusters were estimated from the X-ray diffraction patterns as ranging from 1.3 to 23.1 nm, depending on the annealing temperatures. It was also shown that  $\gamma$ -Fe<sub>2</sub>O<sub>3</sub> transitioned to  $\alpha$ -Fe<sub>2</sub>O<sub>3</sub> at higher annealing temperatures. It is known that magnetic particles consisting of a single domain exhibit superparamagnetic behavior without coersivity below the Curie temperature. However, remarkably large coersivity of about 1 kOe was observed under the appropriate conditions in the above-mentioned nanoparticles, even at room temperature.

In order to improve magnetic parameters such as saturation magnetization ( $M_s$ ) or coersivity ( $H_c$ ), Co<sup>2+</sup> ions were doped into Fe<sub>2</sub>O<sub>3</sub> nanoparticles.

### 2. EXPERIMENTAL

Co doped nanoparticles were prepared by mixing iron chloride FeCl<sub>2</sub>·4H<sub>2</sub>O aqueous solutions, cobalt chloride CoCl<sub>2</sub>·6H<sub>2</sub>O aqueous solutions and sodium metasilicate nonahydrate Na<sub>2</sub>SiO<sub>3</sub>·9H<sub>2</sub>O solutions. The mole ratio of Co/Fe was controlled between 0.05 and 0.7. Controlled mol ratios of Co/Fe for samples were 0.05, 0.125, 0.25, 0.4, 0.5, 0.7 and 1, and these samples were called group (a), (b), (c), (d), (e), (f) and (g), respectively. The resulting precipitates were washed several times with distilled water and dried at about 350 K in a water bath. The dark brown colored glassy solids obtained were calcined between 1073 K and 1273 K.

Prepared samples were examined by X-ray powder diffraction measurements and chemical analysis, and then the magnetization measurements were performed by using a SQUID magnetometer (Quantum Design's MPMS) under an external field between -50 kOe and 50 kOe in the temperature range from 5 K to 300 K.

### 3. RESULTS AND DISCUSSION

#### 3.1 X-ray analysis

X-ray powder diffraction measurements were performed on all samples, and crystal structure, lattice constants and particle size were compared. In the Fe-O system [8], namely the system without Co ions,  $\gamma$ -Fe<sub>2</sub>O<sub>3</sub> with a diameter of 2.2 nm was found in the sample annealed at 923 K. Both  $\gamma$ -Fe<sub>2</sub>O<sub>3</sub> and  $\alpha$ -Fe<sub>2</sub>O<sub>3</sub> with diameters of approximately 4 nm were found at 1073 K, and bulk  $\alpha$ -Fe<sub>2</sub>O<sub>3</sub> crystals were seen at 1173 K. However, doping with Co<sup>2+</sup> ions seemed to repress the bulk crystallization of  $\alpha$ -Fe<sub>2</sub>O<sub>3</sub>. For example, at a doping ratio of 0.125, remaining  $\gamma$ -Fe<sub>2</sub>O<sub>3</sub> nanoparticles with diameters of 5.3 nm were found even annealed at 1173 K.

Fig. 1 shows X-ray diffraction patterns of the sample (d) group (Co/Fe=0.4) being annealed at temperatures of

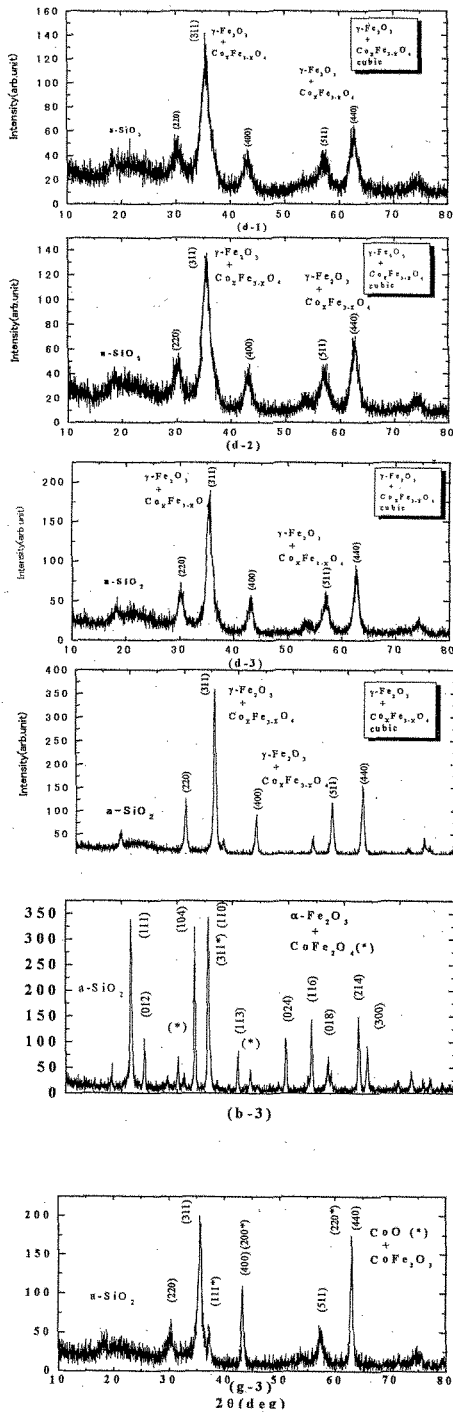


Fig. 1. Powder X-ray diffraction patterns of the sample (d) group (Co/Fe=0.4) being annealed temperature of 1073 K (d-1), 1123 K (d-2), 1173 K (d-3) and 1273 K (d-4), respectively. The latter two patterns of (b-3), in which  $\alpha$ -Fe<sub>2</sub>O<sub>3</sub> and Co-ferrite phases are observed, and (g-2), in which CoO and Co-ferrite phases are observed, are added for the comparison.

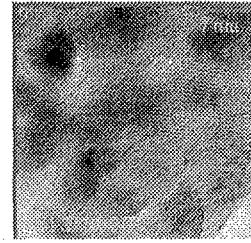


Fig. 2. TEM image of sample (d-3). Guide indicator in the picture is 7 nm.

Table I

Co/Fe	annealing temp.	d (nm)	a (nm)
0.05	923 K	2.4	0.836
	(a) 1073 K	3.9	0.833
	1123 K	7.8	0.841
0.125	1073 K	4.5	0.841
	(b) 1173 K	5.3	0.849
0.25	923 K	2.6	0.838
	(c) 1073 K	4.3	0.833
	1123 K	5.7	0.833
0.4	1073 K	5.1	0.841
	(d) 1123 K	5.5	0.842
	1173 K	7.1	0.832
0.5	1073 K	4.9	0.842
	(e) 1123 K	5.7	0.840
	1173 K	6.6	0.840
0.7	1073 K	5.2	0.838
	(f) 1123 K	6.7	0.839
	1173 K	9.7	0.838
1.0	1073 K	6.1	0.838
	(g) 1123 K	6.2	0.840
	1173 K	8.6	0.835

Table I : Particle sizes of the samples at various concentrations, annealing temperatures with lattice constants estimated by X-ray diffraction.

1073 K (d-1), 1123 K (d-2), 1173 K (d-3) and 1273 K (d-4). From the half widths of the peak intensities, the diameters of the particles can be roughly estimated as 5.1 nm, 5.5 nm, 7.1 nm and 13.8 nm, respectively. The particle sizes estimated in this way have good agreement with the TEM image given in Fig. 2. It can be seen that the mixed spinel ferrite of  $\gamma$ -Fe<sub>2</sub>O<sub>3</sub> and CoFe<sub>2</sub>O<sub>4</sub> are formed in amorphous SiO<sub>2</sub> for c-1, -2, and -3 samples. The d-4 sample shows almost exclusively bulk crystal of  $\gamma$ -Fe<sub>2</sub>O<sub>3</sub>, CoFe<sub>2</sub>O<sub>4</sub> and SiO<sub>2</sub>. Concentrations, annealing temperatures, particle sizes and lattice constants are summarized in Table I.

Larger particles annealed above 1173 K are omitted from the table.

Based on these values, correlation of particle sizes, annealing temperatures and concentrations are shown in Fig. 3.

As an overall tendency, particle sizes grow larger as the annealing temperature increases for each concentration. However, higher concentrations of Co ions seem to repress the crystallization and retain nanosizing.

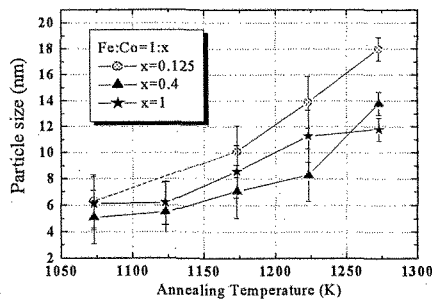
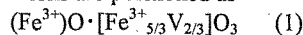


Fig. 3. Correlation of particle sizes, annealing temperatures and concentrations for Co/Fe=0.125 (circle), 0.4 (triangle) and 1 (star), respectively

### 3.2 Magnetic structures

$\alpha$ -Fe<sub>2</sub>O<sub>3</sub> (Hematite) is known to be weak ferromagnetically coupled below  $T_c=958$  K and reordered antiferromagnetically below  $T_M=260$  K. Small hysteresis and  $M_s$  of the  $x=0.05$  sample could be explained by the magnetization of  $\alpha$ -Fe<sub>2</sub>O<sub>3</sub> being dominant in this region. In the  $x=0.4$  sample, both  $\gamma$ -Fe<sub>2</sub>O<sub>3</sub> and CoFe<sub>2</sub>O<sub>4</sub> phases were observed.

$\gamma$ -Fe<sub>2</sub>O<sub>3</sub> (Maghemite) has a cubic inverse spinel of MgAlO<sub>4</sub> crystal type with a lattice constant of  $a=0.8322$  nm. The Fe ions are positioned as



where V shows a vacancy. It is ferrimagnetically ordered below the Curie temperature of  $T_c=1020$  K. (A) site and [B] site are distinguished by different types of brackets.

CoFe<sub>2</sub>O<sub>4</sub> crystallizes in a partially inverse spinel structure represented as  $(\text{Fe}^{3+})[\text{Fe}^{3+}\text{Co}^{2+}]_O_4$ . It is ferrimagnetic below  $T_c=793$  K and shows a relatively large magnetic hysteresis [9]. The critical single domain size of Co-ferrite is reported to be in the order of 70 nm and the superparamagnetic threshold is about 10 nm [10,11]. The maximal coercive force could be attributed to these two ferrimagnetic phases. At a higher concentration of Co ions, the CoO phase was observed as well as CoFe<sub>2</sub>O<sub>4</sub>. A lack of further increase in coercivity with increasing Co content after the maximum value had been reached could be due to the antiferromagnetism of the CoO particles.

### 3.3 Magnetization measurements

Fig. 4 shows the temperature dependence of magnetization (both Field-Cooled and Zero-Field-Cooled) for each concentration being annealed at 1073 K under the field of 1000 Oe, where  $x$  indicates the amount ratio of Co/Fe. All of these particles could be considered to form a single domain and indicate superparamagnetic behavior below  $T_c=1020$  K for  $\gamma$ -Fe<sub>2</sub>O<sub>3</sub> and  $T_c=520$  K for CoFe<sub>2</sub>O<sub>4</sub>. If we define the bifurcated temperature of FC and ZFC as blocking temperature  $T_b$ ,  $T_b$  was found to be 105 K for the ratio  $x=0.05$ , where  $x$  indicates the mole ratio of Co/Fe, 195 K for  $x=0.125$ , 195 K for  $x=0.25$ , 225 K for  $x=0.4$ , 190 K for  $x=0.5$  and 180 K for  $x=0.7$ , respectively. At the blocking temperature,

superparamagnetic spins in a cluster are supposed to be blocked against thermal fluctuation energy.

The magnetization value increased as the proportion of Co ions increased, up to a concentration of  $x=0.4$ , and then at higher concentrations it decreased again and was not proportional to ionic concentration.

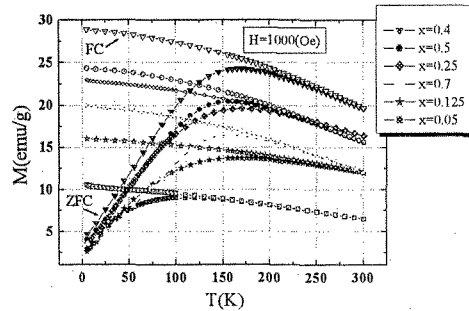


Fig. 4. Temperature dependence of magnetization of FC (open marks) and ZFC (closed marks) for each concentration being annealed at 1073 K under the field of 1000 Oe.

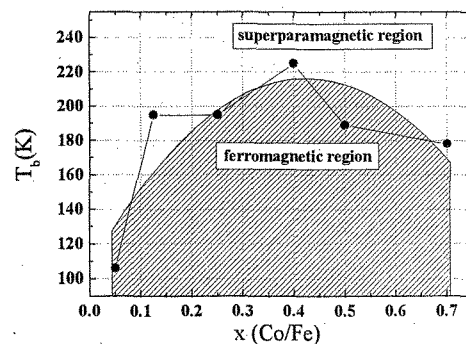


Fig. 5. Concentration dependence of  $T_b$  for the samples annealed at 1073 K. Oblique lines showed ferromagnetic behavior and the region above it showed superparamagnetic behavior.

The concentration dependence of  $T_b$  is summarized in Fig. 5. The region below the  $T_b$ - $x$  curve, indicated by oblique lines, showed ferromagnetic behavior and the region above it showed superparamagnetic behavior. The maximum  $T_b$  was found where Co/Fe equals 0.4.

$M$ - $H$  curves for each concentration annealed at 1073 K are also given in Fig. 6. Samples were measured at a temperature of 100 K, as comparisons between magnetic parameters were clear at that temperature. The magnetization behavior of the sample with  $x=0.05$  was ferromagnetic with extremely slight hysteresis of  $H_c = 380$  Oe and a small saturation magnetization of  $M_s = 18$  emu/g. Hysteresis was shown clearly from  $x=0.125$ , with coercivity of 1010 Oe; and values of  $x=0.25$ , 0.4, 0.5 and 0.7 exhibited coercivity values of  $H_c=1500$ , 1600, 1520 and 1620 Oe, respectively. An enlargement of the part near zero field is shown within Fig. 6.  $\alpha$ -Fe<sub>2</sub>O<sub>3</sub> nanoparticles and a small amount of CoFe<sub>2</sub>O<sub>4</sub> were observed in the X-ray diffraction pattern of the  $x=0.05$  sample.

The concentration dependence of  $H_c$  and  $M_s$  at 100 K,

and expected phases at each region, are summarized in Fig. 7.

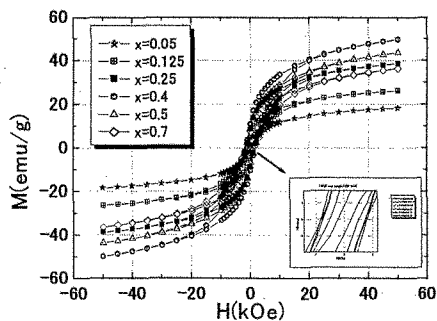


Fig. 6. M-H curves for each concentration annealed at 1073 K.

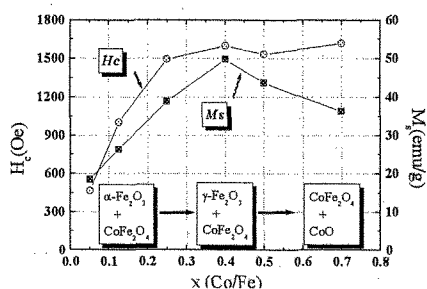


Fig. 7. Concentration dependence of coercivity ( $H_c$ ) and saturation magnetization ( $M_s$ ) at 100 K and expected phases at each region.

### 3.4 Magnetic parameters depending on particle size.

Fig. 8 shows the variations in the coercive field  $H_c$  of the nanoparticle systems annealed between 1073 K and 1123 K as function of their mean diameter size.  $H_c$  increases as the particle sizes increase. Higher concentrations of Co ions tend to suppress the growing particles.

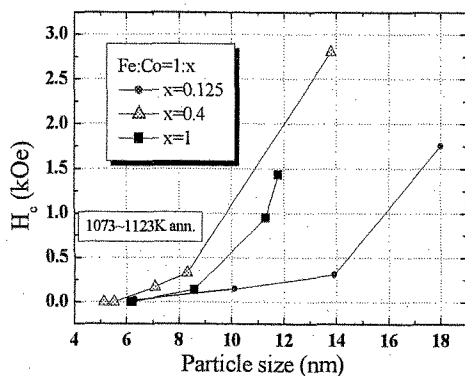


Fig. 8. Variations in the coercive field  $H_c$  of the nanoparticle systems annealed between 1073 K and 1123 K as function of their mean diameter size.

### Conclusion

Co ions were doped into  $\text{Fe}_2\text{O}_3$  nanoparticles. Magnetic parameters changed drastically according to the Co ion content. The coercive force  $H_c$  increased as the annealing temperature increased for all samples, however, particle sizes grew larger than several nanometers. Doping with Co ions seemed to suppress the crystallization of  $\alpha$ - and  $\gamma$ - $\text{Fe}_2\text{O}_3$  nanoparticles. The optimal magnetic parameter value was obtained when the mole ratio of Co/Fe was equal to 0.4 for the sample annealed at 1223 K, at a measuring temperature of 100 K.  $\text{CoFe}_2\text{O}_4$  should be dominant in this composition. Further magnetic properties with higher concentrations of Co ion and in the Co-end region will be reported in the near future.

### Acknowledgements

The authors wish to thank Ms. K.Yabuta, Mr. S.Konuma and Mr. M.Uzaki of KTF for taking TEM images and Ms. Y.Itoh for chemical analysis of the Fe-Co-O nanoparticle system. This study was partially supported by the Japan Society for the Promotion of Science Grant-in Aid for Scientific Research (No. 12650008) and the Yokohama National University Eco-technology System Laboratory.

### References

- [1] Y. Ichiyanagi, Y. Kimishima, *J.Magn.Magn.Mater.*, **140-144**, 1629-1630(1995).
- [2] Y. Ichiyanagi, Y. Kimishima, *Jpn.J.Appl.Phys.*, **35**, 2140-2144(1996).
- [3] Y. Ichiyanagi, Y. Kimishima, *Mat.Sci.Eng.*, **A217**, 358-362(1996).
- [4] Y. Ichiyanagi, Y. Kimishima, *J.Magn.Magn.Mater.*, **177-181**,964-965(1998).
- [5] Y. Ichiyanagi, Y. Kimishima, *J.Magn.Magn.Mater.*, **198-199**,197-199(1998).
- [6] T. Enoki, et al., *J. Phys. Soc. Jpn.* **45(5)** 1515-1519, (1978).
- [7] Y. Ichiyanagi, et al., *Physica B* **329-333**, 862-863 (2003).
- [8] Y. Ichiyanagi, T. Uozumi, *Trans. Mater. Research Soc. Jpn.* **26**,1097-1100(2001).
- [9] M. Rajendran et al., *J. Magn. Magn. Mater.*, **232**,71-83(2001)
- [10] D.J. Dunlop, *Philos. Mag. Ser.19*, 329 (1969).
- [11] A.F. Berkowitz, W.J. Schuele, *J. Appl. Phys.* **30** 134S, (1959).

(Received October 8, 2003; Accepted January 29, 2004)